ORNL/CCIP--91/12

DE91 016775

# MONTE CARLO SIMULATION OF A DYNAMICAL FERMION PROBLEM: THE LIGHT $q^2\bar{q}^2$ SYSTEM

G. Grondin



## DISCLAIMER



to be published in

Proceedings of *Conference on Computational Quantum Physics*
Nashville, Tennessee
May 22-25, 1991

ORNL/CCIP/91/12
UTK/91/06
UTPT/91/15

# MONTE CARLO SIMULATION OF A DYNAMICAL FERMION PROBLEM: THE LIGHT $q^2\bar{q}^2$ SYSTEM

G.Grondin
*Department of Physics, University of Toronto,*
*Toronto, Ontario, Canada M5S 1A7*
*and*
*Physics Division and Center for Computationally Intensive Physics,*
*Oak Ridge National Laboratory, Oak Ridge, TN 37831-6373*

We present results from a Guided Random Walk Monte Carlo simulation of the light $q^2\bar{q}^2$ system in a Coulomb-plus-linear quark potential model using an Intel iPSC/860 hypercube. A solvable model problem is first considered, after which we study the full $q^2\bar{q}^2$ system in $(J,I) = (2,2)$ and $(2,0)$ sectors. We find evidence for no bound states below the vector-vector threshold in these systems.

## I. INTRODUCTION

The possible existence of light four-quark resonances ($q^2\bar{q}^2$, also referred to as baryonia) was first suggested in studies of duality diagrams[1] in the late 1960s. Through the 1970s other models, including the MIT bag model[2] and potential models with truncated color degrees of freedom, predicted that a rich spectrum of four-quark resonances should exist. This was not verified experimentally. The unphysical feature of these models was that they did not allow "fall-apart" decays, so that the four-quark system was not allowed to dissociate into two separate $q\bar{q}$ mesons. The binding implicit in the models held the four quarks together as a single system and generated a tower of excited states.

There is however experimental evidence for two multiquark mesons. The $f_0(975)$ and $a_0(980)$ $J^{PC} = 0^{++}$ resonances were discovered in the early 1960s[3], and could not easily be described as $q\bar{q}$ states. These states were unusual because they were just below $K\bar{K}$ threshold and coupled more strongly to strange final states than to nonstrange states, contrary to expectations for $\frac{1}{\sqrt{2}}(u\bar{u} \pm d\bar{d})$ $^3P_0$ $q\bar{q}$ mesons. Following early suggestions by Jaffe and Johnson[4] that these might be four-quark baryonium

states, Weinstein and Isgur[5] used the nonrelativistic quark model[6] in a variational calculation of the four-quark system in spin-0, isospin-0 and -1 sectors, which led them to identify the $f_0(975)$ and $a_0(980)$ with the loosely-bound $K\bar{K}$ states found in this calculation. Other theoretical and experimental work (for example two-photon decays[7]) also supported this conclusion. Weinstein and Isgur also found that the light $q^2\bar{q}^2$ system in the spin-0 sector had no excited metastable states above these "$K\bar{K}$ molecules" other than the two-meson continuum, which explained why no other four-quark states were seen experimentally.

Approximate solutions of QCD and the four-quark problem have of course been attempted using other methods. One very promising approach is lattice QCD, which simulates the full theory in terms of the QCD Lagrangian on a space-time lattice. This lattice formulation can be studied using Monte Carlo methods to estimate the masses of low-lying states such as the $\pi$, $\rho$, and glueballs. However, these algorithms suffer from a nonlocal equivalent action when applied to dynamical fermions; this leads to slow updates and relatively noisy simulations. The accuracy required to measure the small binding energies expected if the four-quark ground state is a "molecule" of two mesons (perhaps a few tens of $MeV$s) are not yet attainable using unquenched QCD simulations.

Y.G.Liang *et al*[8] used lattice QCD Monte Carlo to search for light $q^2\bar{q}^2$ resonances below vector-vector thresholds in $(J,I) = (0,0)$, $(0,2)$, $(2,0)$, and $(2,2)$. Although they found possible evidence for a bound state in the $(J,I) = (0,0)$ sector, they noted that its mass equals their $\pi\pi$ threshold energy and hence may be an artifact due to transitions to $\pi\pi$ states. Their lattice was modest in size at only $16^3 \times 24$ sites and their quark masses were heavy compared to the physical situation. This demonstrates some useful properties of simulating a Hamiltonian potential model. In a potential model, we can set various Hamiltonian terms to zero to prevent transition to unwanted states and our quark masses can easily be set to currently accepted values.

Another approach, which we follow in the present work, is to attempt a Monte Carlo simulation of "QCD-inspired" potential models, which are based on phenomenological interquark potentials and nonrelativistic dynamics. Since these models are not equivalent to QCD, care must be taken to insure that the relevant physics is incorporated, following which the model predictions can then be tested by comparison with the experimental spectrum of resonances.

Other Monte Carlo studies of the four-quark system in potential models have appeared in the literature, albeit with important simplications. Carlson, Heller, and Tjon[9] studied four-quark systems in which the two quarks were heavy ($c$ and $b$) and the antiquarks were light ($\bar{u}$ and $\bar{d}$). They carried out a Green's Function Monte

Carlo (GFMC) simulation of the Born-Oppenheimer approximation to the bag model and found that the four-quark system was lighter than two separate mesons (*i.e.* a bound state is present). Note however that the four-quark system was again not allowed to decay into two mesons by their Ansatz – this is what originally led to the erroneous prediction of many four-quark resonances. Carlson and Pandeharipande[10] used Variational Monte Carlo and GFMC to study light ($u$ and $d$) multiquark states in a strong-coupling QCD flux-tube potential model. They found no bound states, not even for six quarks; since the deuteron exists, their results imply that either their QCD flux-tube model is an inadequate description of multiquark states or their solution is inaccurate. A possible source of error is that this model mixes the two distinct color basis states only at fourth order in the flux-tube breaking Hamiltonian. This mixing between color ground-state basis vectors may be too weak, so that one finds no binding in systems with more than three quarks. (This problem does not arise in meson and baryon states, which have unique color states.)

In the next section we briefly describe the QCD-inspired quark potential model and discuss some of the relevant physics of the four-quark system. This is followed by a description of the Guided Random Walk (GRW) Monte Carlo algorithm and the modifications which we implemented for our simulation of dynamical fermions. In the fourth section, a simple model Hamiltonian will be introduced and solved as a test case, following which we quote results for the full four-quark problem.

## II. THE HAMILTONIAN

We employ a QCD-inspired quark potential model which has been very successful in describing meson and baryon physics[6,11]. The success of Weinstein and Isgur's description of the $f_0(975)$ and $a_0(980)$ as $K\bar{K}$ bound states also motivates further study of the model as applied to $q^2\bar{q}^2$ states. The Hamiltonian is given by

$$H = \sum_{i=1}^{4}(m_i + \frac{P_i^2}{2m_i}) + \sum_{i<j}(V_{conf}^{ij} + V_{eff}^{ij}), \tag{1}$$

where

$$V_{conf}^{ij} = -(C + \frac{3}{4} b\, r_{ij})\, \vec{F}_i \cdot \vec{F}_j \tag{2}$$

contains constant and linear confining terms, and

$$V_{eff}^{ij} = V_{Coul}^{ij} + V_{hyp}^{ij} + V_{so}^{ij} \tag{3}$$

is a one-gluon-exchange term with

$$V_{Coul}^{ij} = \frac{\alpha_s}{r_{ij}}\, \vec{F}_i \cdot \vec{F}_j \tag{4}$$

and

$$V^{ij}_{hyp} = \frac{\alpha_s}{m_i m_j}\left[\frac{8\pi}{3}\vec{S}_i\cdot\vec{S}_j\,\delta^3(r_{ij}) + V^{ij}_{ten}\right]\vec{F}_i\cdot\vec{F}_j. \tag{5}$$

These terms suffice for a surprisingly accurate description of light nonrelativistic hadron spectroscopy. We choose to neglect the usually unimportant tensor and spin-orbit terms, $V^{ij}_{ten}$ and $V^{ij}_{so}$, because their contribution to a dominantly S-wave ground state is expected to be much smaller than that of the spin-spin term.

Since we are simulating a Schrödinger equation numerically, the delta-function must be smoothed if we are to obtain a physically realistic spectrum. Our replacement

$$\delta^3(r_{ij}) \longrightarrow \frac{\sigma_{hf}^3}{\pi^{3/2}}\exp(-\sigma_{hf}^2 r_{ij}^2) \tag{6}$$

can also be motivated as a "smearing" of the delta-function caused by Zitterbewegung. It is also necessary to regulate the color Coulomb term $V^{ij}_{Coul}$ at contact. We substitute

$$\frac{1}{r} \longrightarrow \begin{cases} \frac{1}{r} & r > h_x \\ \frac{1}{h_x} & 0 \le r \le h_x \end{cases} \tag{7}$$

where $h_x$ is the spatial lattice size, which we subsequently extrapolate to zero.

For the present we consider only light $u$ and $d$ quarks in the equal-mass limit. We must construct totally antisymmetric four-quark states, which are products of spatial ($\psi$), spin ($\chi$), flavor ($\phi$), and color ($C$) wavefunctions. Each carries a subscript S or A, which denotes a symmetric or antisymmetric state under exchange of quarks (labelled 1 and 2) or antiquarks (labelled 3 and 4).

There are two "natural" color bases which we might employ (see Figure 1). The $(|1_{13}1_{24}\rangle, |1_{14}1_{23}\rangle)$ basis corresponds to the "color flux lines" that can be drawn for a system of two separate mesons; this is the more physical basis if we expect the four-quark system to be molecule-like or unbound. These two $|1,1\rangle$ basis states are not orthogonal in color space, and this complication leads to nondiagonal kinetic terms which are not easily simulated by the GRW algorithm. We therefore use the orthogonal basis $(|\bar{3}_{12}3_{34}\rangle, |6_{12}\bar{6}_{34}\rangle)$ in which the fermion symmetry is explicit; interpretation of the results in terms of color-singlet meson states is, unfortunately, rather more difficult in this basis. The relation between the two bases is

$$|1_{13}1_{24}\rangle = \sqrt{\frac{1}{3}}\,|\bar{3}_{12}3_{34}\rangle + \sqrt{\frac{2}{3}}\,|6_{12}\bar{6}_{34}\rangle, \tag{8}$$

$$|1_{14}1_{23}\rangle = -\sqrt{\frac{1}{3}}\,|\bar{3}_{12}3_{34}\rangle + \sqrt{\frac{2}{3}}\,|6_{12}\bar{6}_{34}\rangle.$$

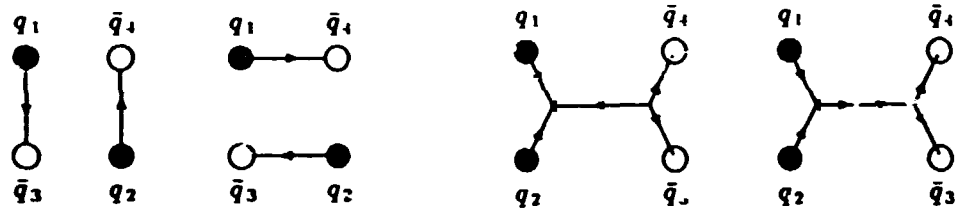


FIG. 1. Color bases.

From four spin-$\frac{1}{2}$ objects with no orbital excitation we can construct states with total spin $J = 0, 1$ and 2. We neglect orbital angular momentum in listing the possible $J$ values because dominantly S-wave bound states are most likely *a priori*. We shall first consider the $J = 2$ case. These states have a symmetric spin wavefunction $\chi_S$, and are diagonal in the spin-spin Hamiltonian,

$$\vec{S}_i \cdot \vec{S}_j |J = 2, J_m\rangle = \frac{\hbar^2}{4} |J = 2, J_m\rangle . \tag{8}$$

The flavor wavefunctions have total isospin $I = 0$, 1, or 2. Here we consider only $I = 0$ and $I = 2$, which are totally symmetric or antisymmetric under identical fermion exchange. The $I = 1$ states, in contrast, have opposite exchange symmetry for the quarks and antiquarks. This more complicated symmetry requires a more complicated spatial wavefunction to maintain the overall fermion antisymmetry. (The color and spin states are already fixed.)

Finally, the spatial wavefunction $\psi(\vec{x}, \vec{y}, \vec{z})$ can be shown to have definite symmetry in $\vec{x}$ and $\vec{y}$ under identical fermion exchange. Figure 2 shows the definition of these Weinstein-Isgur coordinates; the center-of-mass coordinate can be factored out of the Hamiltonian and need not be considered. The separation between the center-of-mass coordinates of specified $q\bar{q}$ pairs is given by the coordinate $\vec{x}$ (or $\vec{y}$); if the two-meson system is unbound, then the expected $\vec{x}$ or $\vec{y}$ must diverge.

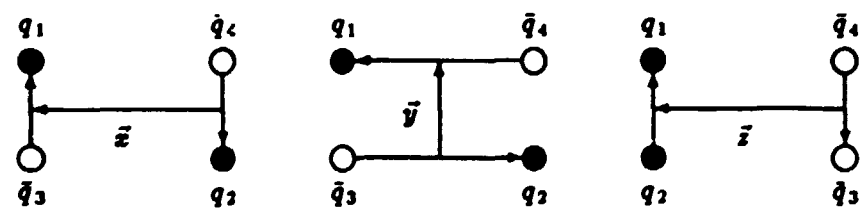


FIG. 2. Spatial coordinates.

To illustrate the spatial symmetry of $\psi$, consider the $(J,I) = (2,2)$ system; we specialize to the $\rho^+\rho^+$ sector, which has flavor and spin states $|\phi_S\rangle = |uu\bar{d}\bar{d}\rangle$ and $|\chi_S\rangle = |\uparrow\uparrow\uparrow\uparrow\rangle$. One might *a priori* consider writing the state as $\psi(\vec{x},\vec{y},\vec{z})|1_{13}1_{24}\rangle$, but this does not give a correctly symmetrized state. If we apply identical-fermion exchange symmetry to the ground-state wavefunction (which we denote by $|\rho^+\rho^+\rangle$ for simplicity), we can rewrite it as

$$|\rho^+\rho^+\rangle = \Big(\psi(\vec{x},\vec{y},\vec{z}) + \psi(-\vec{x},-\vec{y},\vec{z})\Big)|1_{13}1_{24}\rangle \pm \Big(\psi(\vec{y},\vec{x},\vec{z}) + \psi(-\vec{y},-\vec{x},\vec{z})\Big)|1_{14}1_{23}\rangle; \tag{10}$$

the $\pm$ determines the symmetry of the wavefunction under exchange of one pair of quarks or antiquarks. For $|\rho^+\rho^+\rangle$ we must chose the minus sign but in the $(J,I) = (2,0)$ sector we can find an antisymmetric flavor function which allows the positive sign. For the negative case in (10) we can rewrite the state as

$$|\rho^+\rho^+\rangle = \sqrt{\frac{1}{3}}\,\psi_S(\vec{x},\vec{y},\vec{z})|\bar{3}_{12}3_{34}\rangle + \sqrt{\frac{2}{3}}\,\psi_A(\vec{x},\vec{y},\vec{z})|6_{12}\bar{6}_{34}\rangle. \tag{11}$$

This uses the color basis $(|\bar{3}_{12}3_{34}\rangle, |6_{12}\bar{6}_{34}\rangle)$ and introduces the symmetrized combinations

$$\psi_S(\vec{x},\vec{y},\vec{z}) \equiv \Big(\psi(\vec{x},\vec{y},\vec{z}) + \psi(-\vec{x},-\vec{y},\vec{z})\Big) + \Big(\psi(\vec{y},\vec{x},\vec{z}) + \psi(-\vec{y},-\vec{x},\vec{z})\Big), \tag{12}$$

$$\psi_A(\vec{x},\vec{y},\vec{z}) \equiv \Big(\psi(\vec{x},\vec{y},\vec{z}) + \psi(-\vec{x},-\vec{y},\vec{z})\Big) - \Big(\psi(\vec{y},\vec{x},\vec{z}) + \psi(-\vec{y},-\vec{x},\vec{z})\Big).$$

Equation (12) explicitly shows the symmetry of $\psi_S$ and $\psi_A$ under $(\vec{x},\vec{y})$ interchange, and also shows that $\psi_S(\vec{x},\vec{y},\vec{z}) = \psi_S(-\vec{x},-\vec{y},\vec{z})$ and $\psi_A(\vec{x},\vec{y},\vec{z}) = \psi_A(-\vec{x},-\vec{y},\vec{z})$.

## III. THE GUIDED RANDOM WALK ALGORITHM

The guided random walk (GRW) Monte Carlo algorithm was introduced by Barnes, Daniell, and Storey[12] as an alternative to branching algorithms. The earlier versions of GRW considered systems having either continuous[12] or discrete[13] degrees of freedom but did not consider systems with both in the same Hamiltonian (for a summary of both versions see Barnes[14]). The modified GRW algorithm presented here allows the simulation of systems having both types of state.

First consider an unguided RW method based on a Euclidean form of the Schrödinger equation; on taking $it \to \tau$ it becomes a diffusion equation,

$$-\hbar\frac{\partial}{\partial\tau}\,|\psi(\tau)\rangle = H\,|\psi(\tau)\rangle\,. \tag{13}$$

Such a diffusion equation can then be simulated by generating random walks on a space-time lattice (Figure 3), as first proposed by E.Fermi[15], and weighting each walk with an appropriate factor. (This is similar to the $e^{-S}$ weight in path integrals.) In the limit $h_x$, $h_\tau \to 0$ with $h_\tau / h_x^2$ constant, the weighted RW process can be made equivalent to the diffusion process (13). In a simulation of the diffusion equation (13), the ground-state wavefunction and energy are generated in the large-$\tau$ limit, as can be seen from an eigenmode expansion of the initial wavefunction. We assume that the initial wavefunction has a nonzero overlap with the true ground state,

$$|\psi(0)\rangle = \sum_n c_n |\psi_n\rangle , \tag{14}$$

so that

$$|\psi(\tau)\rangle = \sum_n c_n |\psi_n\rangle e^{-E_n \tau}, \tag{15}$$

which implies

$$\lim_{\tau \to \infty} |\psi(\tau)\rangle = c_0 e^{-E_0 \tau} |\psi_0\rangle + O(e^{-(E_1 - E_0)\tau}). \tag{16}$$

An unweighted random walk simulates a diffusion equation with no potential. To include a potential, each walk is given a weight which is determined by the potential $V$ and the path of the walk. The ground-state energy and wavefunction are found using the expected weight and a weight-factor histogram. In the unguided algorithm these weights have widely scattered values (again see Barnes[14]); the wider the scatter of the weights, the greater the computational effort required to achieve a prescribed statistical accuracy.

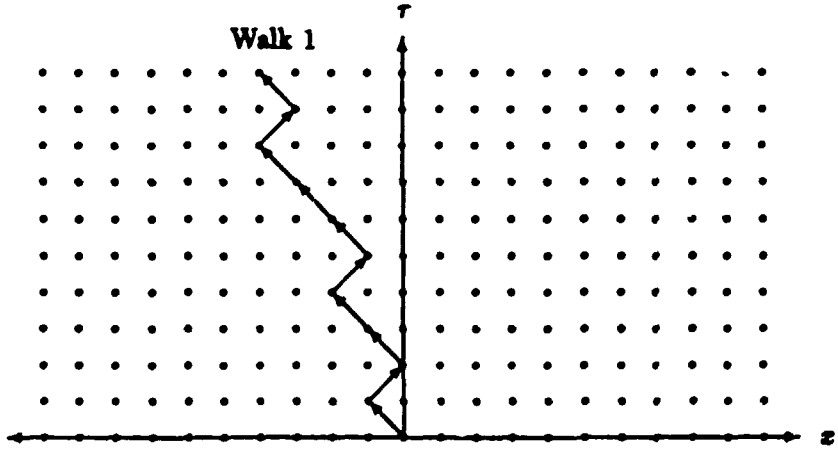


FIG. 3. A random walk on the lattice.

The GRW algorithm attempts to improve the statistical accuracy by introducing a trial "guiding" wavefunction, which guides the walks into regions where the ground-state $\psi_0$ is expected to be large. The guiding wavefunction does not introduce a bias in the determination of the ground-state energy or matrix elements, since a generalized weight is introduced which compensates for the effects of the guidance. Formally the algorithm used here is essentially that of Barnes and Daniell[13]; only a few changes are required for our simulation.

The walk is performed on a lattice (with coordinate resolution $h_x$) in the configuration space $Z = (x_i, S)$; $x_i$ is the $q^2\bar{q}^2$ $(\vec{x}, \vec{y}, \vec{z})$ coordinate space, and $S$ is the color $\otimes$ isospin $\otimes$ spin state (only two such states are present). At each time step $h_\tau$, the probability to go from $Z$ at time $\tau$ to $Z'$ at time $\tau + h_\tau$ is written as

$$p_{Z\to Z'} = r_{Z\to Z'}\, h_\tau \tag{17}$$

with $h_\tau$ determined from conservation of probability,

$$\sum_{Z'} p_{Z\to Z'} = 1. \tag{18}$$

Each walk is assigned a weight factor $W_{tot}$ which is given by

$$\begin{aligned} W_{tot} &= W_{diag} \cdot W_{tran}, \\ W_{diag} &= \exp\left\{ -\int_0^\tau \left( V_0(Z(\tau')) - \sum_{Z'\neq Z} r_{Z\to Z'} \right) d\tau' \right\}, \\ W_{tran} &= \prod_{\substack{\text{transitions} \\ Z\to Z'\neq Z}} \left( -\frac{\langle Z'|\, H_I \,|Z\rangle}{r_{Z\to Z'}} \right), \end{aligned} \tag{19}$$

where $H = H_0 + H_I$, and $H_0(Z) \equiv V_0(Z) = \langle Z|\, H_0 \,|Z\rangle$. (By definition $H_0$ is diagonal and $H_I$ is off-diagonal in state space.)

Previously Barnes[14] chose to specialize $r_{Z\to Z'}$ to a particular form in terms of a "guiding wavefunction" $\psi_g$,

$$r_{Z\to Z'} = -\langle Z'|\, H_I \,|Z\rangle \frac{\psi_g(Z')}{\psi_g(Z)}. \tag{20}$$

This form simplifies $W_{tran}$, and in the "perfect guidance" case in which $\psi_g$ is equal to the true ground-state wavefunction, sets the diagonal weight exactly equal to $\exp(-E_0\tau)$. As the energy is determined from the $\tau$-dependence of $W_{tot}$, equation (20) makes $W_{tran}$ a function of $Z$ only, and it can therefore be discarded in energy measurements. In practice, the true ground-state wavefunction is not known and is approximated by a parametrized guiding wavefunction $\psi_g$; we then vary the

parameters of $\psi_g$ and search for a minimum of the variance of the diagonal weights. (Zero variance in $W_{diag}$ indicates that $\psi_g$ actually equals an energy eigenstate wavefunction.) In this $q^2\bar{q}^2$ problem, however, the right hand side of (20) is not always positive definite, whereas the stepping probability $r_{Z\to Z'}h_\tau$ must be. To force $r_{Z\to Z'}$ to be positive we instead choose

$$r_{Z\to Z'} = \left| -\langle Z'|\, H_I\, |Z\rangle \frac{\psi_g(Z')}{\psi_g(Z)} \right|, \tag{21}$$

which requires

$$W_{tran} = \left| \frac{\psi_g(Z(0))}{\psi_g(Z(\tau))} \right| \prod_{\substack{transitions \\ Z\to Z'\neq Z}} \mathrm{sign}\left(-\langle Z'|\, H_I\, |Z\rangle\right). \tag{22}$$

This form allows a dynamical generation of the wavefunction's nodal structure, since both positive and negative weights are generated by the algorithm if some $\langle Z'|\, H_I\, |Z\rangle$ matrix elements are positive. It also retains the zero-variance property for $\psi_g = \psi_0$ which $r_{Z\to Z'}$ defined by (20) possessed for negative definite or zero $\langle Z'|\, H_I\, |Z\rangle$.

The ground-state energy is estimated from the $\tau$-dependence of the average sign-weighted diagonal weight

$$\left\langle W_{diag}\,\mathrm{sign}(W_{tran})\right\rangle = \frac{1}{N_{rw}} \sum_{i}^{N_{rw}} \left\{ W^i_{diag} \prod_{\substack{i\,transitions \\ Z\to Z'\neq Z}} \mathrm{sign}\left(-\langle Z'|\, H_I\, |Z\rangle\right) \right\}; \tag{23}$$

$$\lim_{\tau\to\infty} \left\langle W_{diag}(\tau)\,\mathrm{sign}(W_{tran})\right\rangle \propto \exp(-E_0\tau). \tag{24}$$

Unbiased matrix elements can in principle be determined from $W_{tot}$ (see Barnes[14]), although we shall only consider energies here.

If we evaluate equation (24) directly, the statistical error in the energy could be large, due to cancellations between negative and positive weights. As the energy is determined from the $\tau$-dependence of the expected weight alone, we can multiply the final histogram of weights by any function of the coordinate $Z$ (which we call a "masking function") to reduce the fraction of negative weights and hence to increase the statistical accuracy in the energy. We normally attempt to approximately reproduce the nodal structure of $\psi_0$ in the masking function. Note however that no bias will result if the nodal structure of the masking function is not identical to that of $\psi_0$. (Actually in this problem we do know the exact nodes, which we will discuss subsequently.)

The implementation of the code is parallel, in that we run $n$ copies of the program, each generates a set of walks on its own "node" (CPU), and the resulting weights are

summed at the end of the run. It is possible to run one program per node because the algorithm has very small memory requirements; this avoids the complications of internode communication.

## IV. RESULTS

Before considering the full Hamiltonian (1), we first consider an analytically-solvable Hamiltonian which is very similar to that introduced by Weinstein and Isgur[5]. Our test problem is defined by

$$\tilde{H}_0 = \left[4m - \frac{\hbar^2}{2m}\left(\nabla^2_{\vec{x}} + \nabla^2_{\vec{y}} + \nabla^2_{\vec{z}}\right) + \frac{1}{2}(2k)(x^2+y^2) + \frac{1}{2}(4k)z^2\right]\begin{pmatrix}1&0\\0&1\end{pmatrix} + \frac{1}{2}k_n(y^2-x^2)\begin{pmatrix}0&1\\1&0\end{pmatrix}, \tag{25}$$

whereas the test problem of Weinstein and Isgur[5] instead substitutes

$$V^{ij}_{conf} + V^{ij}_{eff} \longrightarrow -(C + \frac{4}{3}(\frac{1}{2}k r^2_{ij}))\vec{F}_i \cdot \vec{F}_j, \tag{26}$$

in (1), which produced an intractable Hamiltonian. Our solvable $\tilde{H}_0$ is their (26) without a diagonal term. The energy of a general eigenstate of $\tilde{H}_0$ is

$$E_{ijk} = 4m + \frac{\hbar}{2\sqrt{m}}\left(\sqrt{2k-k_n}(2i_1+2i_2+2i_3+3) + \sqrt{2k+k_n}(2j_1+2j_2+2j_3+3) + \sqrt{4k}(2k_1+2k_2+2k_3+3)\right), \tag{27}$$

where

$$\gamma_1 = \frac{1}{2\hbar}\sqrt{m(2k-k_n)} \tag{28}$$
$$\gamma_2 = \frac{1}{2\hbar}\sqrt{m(2k+k_n)}$$
$$\gamma_3 = \frac{1}{2\hbar}\sqrt{m(4k)}.$$

If we define

$$H_{i;l}(\vec{x}) \equiv H_{i_1}(\sqrt{2\gamma_l}\,x_1)\,H_{i_2}(\sqrt{2\gamma_l}\,x_2)\,H_{i_3}(\sqrt{2\gamma_l}\,x_3), \tag{29}$$

where $H_i(x)$ is a Hermite polynomial, then the energy eigenfunction corresponding to (27) is

$$\left|\psi^{\pm}_{ijk}\right\rangle = \begin{bmatrix} H_{i;1}(\vec{x})H_{j;2}(\vec{y})\exp(-\gamma_1 x^2 - \gamma_2 y^2) \mp H_{j;2}(\vec{x})H_{i;1}(\vec{y})\exp(-\gamma_2 x^2 - \gamma_1 y^2) \\ H_{i;1}(\vec{x})H_{j;2}(\vec{y})\exp(-\gamma_1 x^2 - \gamma_2 y^2) \pm H_{j;2}(\vec{x})H_{i;1}(\vec{y})\exp(-\gamma_2 x^2 - \gamma_1 y^2) \end{bmatrix} \cdot H_{k;1}(\vec{z})\exp(-\gamma_1 z^2). \tag{30}$$

Our test $H_0$ has the same degrees of freedom as the full Hamiltonian (1), and also has terms of either sign off-diagonal, as is expected in a dynamical fermion problem. It also has a "fall apart" solution; the ground-state wavefunction is independent of the relative-separation coordinate $\vec{x}$ when $2k = k_n$.

Figure 4 shows the Euclidean-time dependence of the extracted ground-state energy with a fixed lattice size; in practice we increase $\tau$ until evidence for $\tau$-dependence has disappeared to the required accuracy, which indicates that contributions from excited states have become unimportant. We then extrapolate the energy to zero lattice size at this value of $\tau$, as shown in Figure 5. The algorithm evidently finds the correct ground-state energy to our statistical accuracy of about 0.1 $MeV$. We used $|\psi^{+}_{000}\rangle$ from (30) as our guiding wavefunction for this simulation; this guiding function equals the true ground state only when $h_x = 0$, and we find accordingly that the variance of the diagonal weights does indeed go to zero as $h_x \to 0$.

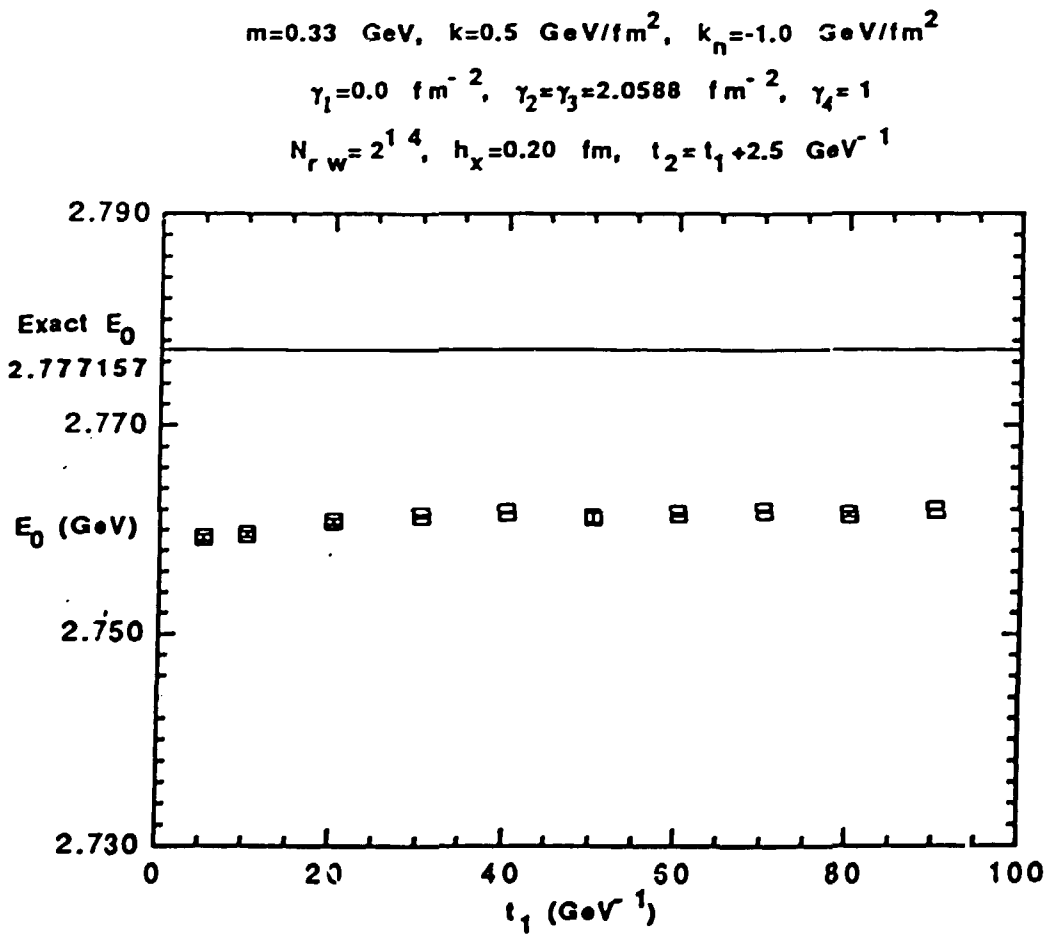


FIG. 4. $E_0(\tau)$ for the analytic test case.
See also the $h_x^2$ extrapolation in Figure 5.

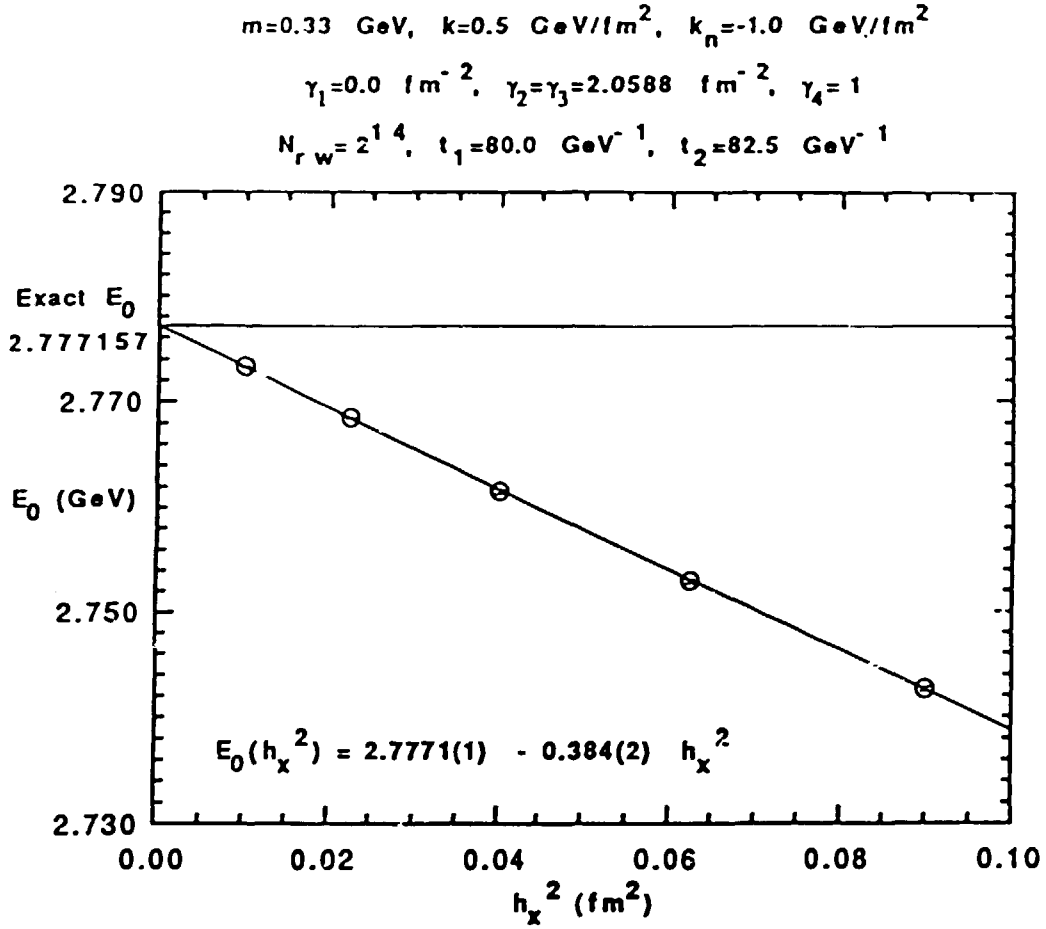


FIG. 5. $E_0(h_x^2)$ for the analytic test case.

One of our principal concerns in solving equation (1) with the GRW algorithm is to insure that $\psi_g$ does not impose an incorrect nodal structure. In a general multifermion problem the nodes are usually unknown. For this problem we can use the eigenfunctions of $\tilde{H}_0$ to exactly determine the nodes of the ground-state eigenfunction of (1).

We will treat (1) as a perturbation $\tilde{H}_I$ about (25); we must restrict the eigenfunction basis set of (30) to eigenfunctions for which $i_1 + i_2 + i_3 + j_1 + j_2 + j_3$ is even, in order to satisfy the constraint $\psi(\vec{x},\vec{y},\vec{z}) = \psi(-\vec{x},-\vec{y},\vec{z})$. Note that $\tilde{H}_I$ can be written as

$$\tilde{H}_I = \begin{bmatrix} f_1(\vec{x},\vec{y},\vec{z}) & f(\vec{x},\vec{y},\vec{z}) \\ f(\vec{x},\vec{y},\vec{z}) & f_2(\vec{x},\vec{y},\vec{z}) \end{bmatrix}, \tag{31}$$

where

$$f_m(\vec{x},\vec{y},\vec{z}) = f_m(-\vec{x},-\vec{y},\vec{z}) \tag{32}$$

$$= f_m(\vec{y}, \vec{x}, \vec{z})$$

and

$$\begin{aligned} f(\vec{x}, \vec{y}, \vec{z}) &= f(-\vec{x}, -\vec{y}, \vec{z}) \\ &= -f(\vec{y}, \vec{x}, \vec{z}). \end{aligned} \tag{33}$$

From this form we can easily show that

$$\langle \psi^-_{ijk} | \tilde{H}_I | \psi^+_{lmn} \rangle = 0. \tag{34}$$

We may now apply perturbation theory in $\tilde{H}_I$ to determine properties of the eigenstates of $\tilde{H}$. Let the eigenstates of $\tilde{H}_0$ be written as $|n^\pm\rangle$ with eigenvalue $E_n(0)$. The eigenstates of $\tilde{H}$ can then be written as

$$E = E(0) + \lambda E(1) + \lambda^2 E(2) + \cdots \tag{35}$$

and

$$|\Psi\rangle = |\Phi_0\rangle + \lambda|\Phi_1\rangle + \lambda^2|\Phi_2\rangle + \cdots, \tag{36}$$

where $|\Phi_0\rangle = |\psi^+_{000}\rangle$ and $\langle \Phi_n | \Phi_0 \rangle = \delta_{n0}\ \forall n$. (We can also determine $|\psi^-_{000}\rangle$ by changing + to − where appropriate.) We need only determine the ground-state wavefunction, since the GRW algorithm converges to that state. The perturbative results for $E$ and $|\Psi\rangle$ are given by

$$E(n) = \langle \Phi_0 | \tilde{H}_I | \Phi_{n-1} \rangle \tag{37}$$

and

$$\begin{aligned} |\Phi_n\rangle = [E(0) - \tilde{H}_0]^{-1} [I - |\Phi_0\rangle\langle\Phi_0|] \big[ [\tilde{H}_I - E(1)] |\Phi_{n-1}\rangle \\ + E(2)|\Phi_{n-2}\rangle + \cdots + E(n-1)|\Phi_1\rangle \big]. \end{aligned} \tag{38}$$

Using (34), we can easily show that the first- and second-order perturbative contributions to the ground-state wavefunction are

$$|\Phi_1\rangle = \sum_{n \neq 0} \frac{|n^+\rangle\langle n^+|\tilde{H}_I|\Phi_0\rangle}{E(0) - E_n(0)} \tag{39}$$

and

$$|\Phi_2\rangle = \sum_{n \neq 0} \sum_{m \neq 0} \frac{|n^+\rangle\langle n^+|(\tilde{H}_I - E(1))|m^+\rangle\langle m^+|\tilde{H}_I|\Phi_0\rangle}{(E(0) - E_n(0))(E(0) - E_m(0))}. \tag{40}$$

Neither of these has a contribution from the $\{|n^-\rangle\}$ states. One may prove by induction that no $|\Psi_n\rangle$ has a contribution from the $\{|n^-\rangle\}$ states[16]. The ground-state wavefunction may therefore be written as

$$|\Psi\rangle = |0^+\rangle + \sum_{n\neq 0} c_n |n^+\rangle. \tag{41}$$

Using (30) and letting $S = \frac{1}{2}(\gamma_2 + \gamma_1)$ and $D = \frac{1}{2}(\gamma_2 - \gamma_1)$, we find that the node in the upper component of (41) is determined by

$$0 = 2\sinh(D(x^2 - y^2)) + \sum_{i,j,k} c_{i,j,k} \left[ H_{i;1}(\vec{x}) H_{j;2}(\vec{y}) \exp(D(x^2 - y^2)) \right.$$
$$\left. - H_{j;2}(\vec{x}) H_{i;1}(\vec{y}) \exp(-D(x^2 - y^2)) \right] H_{k;3}(\vec{z}). \tag{42}$$

As $D \neq 0$ in general, this equation is only satisfied by $\vec{x} \pm \vec{y} = 0$, or equivalently by $x^2 - y^2 = 0$. If we now consider finding the eigenvectors of $\tilde{H}_I$ alone, we can use the eigenfunctions (30) as the basis e genvectors, since they span the configuration sp_ce and satisfy the symmetry requirement (12) for eigenvectors of $\tilde{H}_I$. The ground-state eigenvector can therefore be written in the form (41), which implies that the nodes of the ground-state eigenfunction of (1) are given by $x^2 - y^2 = 0$. This motivates our choice of the ground-state eigenfunction of $\tilde{H}_0$ as the trial wavefunction $\psi_g$ in the simulation of (1), as this $\psi_g$ has this nodal structure.

The Euclidean-time dependence of the ground-state energy estimate for (1) in the $(J, I) = (2, 2)$ sector is shown in Figure 6. The values of the parameters were determined in a fit to light meson spectroscopy[17], and are similar to the conventional quark model values. The lattice energy extrapolation gives a value for the four-quark ground-state energy which equals that of two free mesons to within $\approx 5\,MeV$. Preliminary results for the ground-state energy in the $(J, I) = (2, 0)$ sector leads to a four-quark ground-state energy equal to that of two free mesons to within $\approx 10\,MeV$. Thus we conclude that there are no bound states in the $I = 2$ $(\rho^+\rho^+)$ and $I = 0$ $(\rho\rho + \omega\omega)$ sectors of the nonrelativistic quark potential model to within an accuracy of $10\,MeV$. The former result is consistent with the lattice QCD results of Y.G.Liang *et al*[8] in the $(J, I) = (2, 2)$ sector.

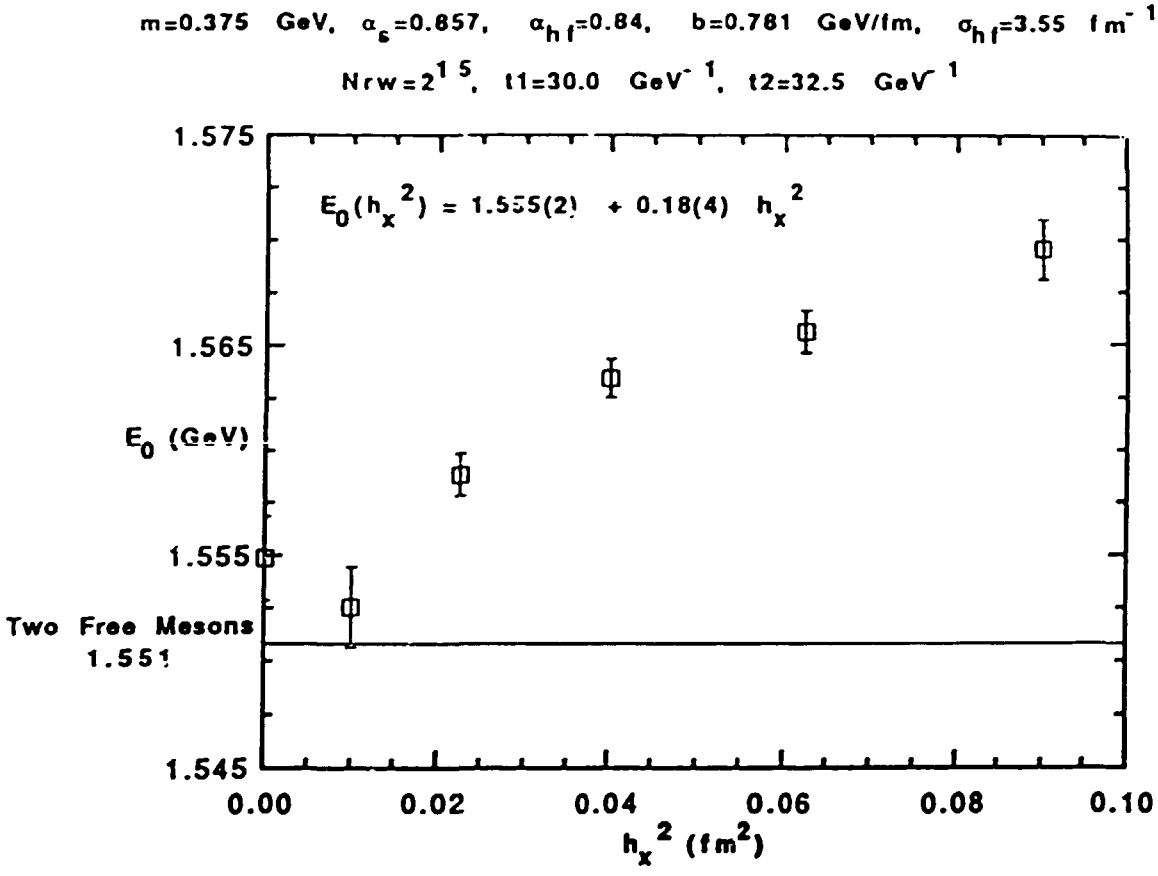


FIG. 6. $E_0(h_x^2)$ in the $(J,I) = (2,2)$ sector ($\rho^+\rho^+$ quantum numbers). The point at the origin is extrapolated from a linear fit in $h_x^2$.

## V. CONCLUSIONS

We have applied an extension of the GRW Monte Carlo algorithm to a dynamical fermion problem, the $q^2\bar{q}^2$ system. The extended algorithm allows the simulation of systems having both continuous and discrete degrees of freedom, and is applicable to Hamiltonians with both positive and negative off-diagonal matrix elements, as characteristically occur in dynamical fermion problems.

We first applied the algorithm to an analytically solvable test problem which has many of the properties of the full four-quark Hamiltonian. From the solution of the test problem we demonstrated that the node of the four-quark ground-state wavefunction is given by $x^2 - y^2 = 0$. Employing this in our choice of guiding wave-

function, we used the Monte Carlo algorithm to estimate the ground-state energies of the $(J, I)$ $(2,2)$ and $(2,0)$ light four-quark systems in a Coulomb-plus-linear quark potential model.

We find evidence for no bound states of two light vector mesons in the channels studied ($J$ 2; $\rho^+\rho^+$, $\rho$ $\rho$ , $\omega\omega$, $\rho \cdot \rho$, ...) in the nonrelativistic quark potential model. The mass of the four-quark state was found to equal that of two free mesons to within our statistical errors of about 5 $MeV$ for $I = 2$ and about 10 $MeV$ for $I = 0$. We hope to improve this measurement in future and to extract an equivalent potential between vector meson pairs, which should be useful in the study of final state interactions in these systems.

## VI. ACKNOWLEDGEMENTS

I would like to thank T.Barnes for his advice and instruction throughout this work. I also thank K.Dooley, E.S.Swanson and J.Weinstein for their discussions of four-quark physics and D.Kotchan and M.Kovarik for helpful discussions of the GRW algorithm. I wish to acknowledge the support and facilities provided by the Physics Department of the University of Toronto, Oak Ridge National Laboratory (in particular the Theory Division and the EPM Division), and the Physics Department of the University of Tennessee. This research was supported in part by grants from the Natural Sciences and Engineering Research Council of Canada and by an E.C.Stevens Fellowship and a Walter C.Sumner Memorial Fellowship and also by the Division of Nuclear Physics, U.S. Department of Energy under Contract No. DE-AC05-84OR21400 managed by Martin Marietta Energy Systems Inc., the Physics Department of the University of Tennessee under Contract No. DE-AS05-76ER03956, and the State of Tennessee Science Alliance Center under Contract No. R01-1062-32. Finally, I thank the organizers of the Conference on Computational Quantum Physics (hosted by the Physics Department of Vanderbilt University, Nashville, Tennessee) for extending an invitation to discuss this material with my fellow participants.

---

[1] J.Rosner, Phys. Rev. Lett. 21, 950 (1968); H.Harari, Phys. Rev. Lett. 22, 562 (1969).

[2] R.L.Jaffe, Phys. Rev. Lett. 38, 195 (1977) and 38, 617(E) (1977); K.Saito, Prog. Theor. Phys. 72, 674 (1984).

[3] T.-T.Wang *et.al.*, JETP 13, 323 (1961) for the $f_0(975)$; F.Turkot *et.al.*, Sienna

Conf. 1, 661 (1963) for the $a_0(980)$.

[6]R.L.Jaffe and K.Johnson, Phys. Lett. 60B, 201 (1977); R.L.Jaffe, Phys. Rev. D15, 267, 281 (1977) and D17, 1444 (1978).

[7]J.Weinstein and N.Isgur, Phys. Rev. Lett. 48, 659 (1982); Phys. Rev. D27 588 (1985).

[8]S.Godfrey and N.Isgur, Phys. Rev. D32, 189 (1985) for mesons; S.Capstick and N.Isgur, Phys. Rev. D34, 2809 (1986) for baryons.

[7]T.Barnes, Phys. Rev. B165, 434 (1985).

[8]Y.G.Liang, B.A.Li, K.F.Liu, T.Draper and R.M.Woloshyn, Proceedings of Int. Conf. "Lattice 89", Capri, 1989, Nucl. Phys. B, Proc. Supplement.

[9]J.Carlson, L.Heller, and J.A.Tjon, Phys. Rev. D37, 744 (1988).

[10]J.Carlson and V.R.Pandharipande, Phys. Rev. D43, 1652 (1991).

[11]N.Isgur and G.Karl, Phys. Rev. D18, 4187 (1978).

[12]T.Barnes, G.Daniell, and D.Storey, Nucl. Phys. B265[FS15], 253 (1986).

[13]T.Barnes and G.J.Daniell, Phys. Rev. B37, 3637 (1988).

[14]T.Barnes, "Numerical Solution of High Temperature Superconductor Spin Systems", p.83, *Nuclear and Atomic Physics at One Gigaflop*, ed. C.Bottcher, M.R.Strayer, and J.B.McGrory (Harwood Academic Publishers, Chur, Switzerland, 1989).

[15]E.Fermi, in N.Metropolis and S.Ulam, J. Am. Stat. Assoc. 247, 335 (1949).

[16]G.Grondin, University of Toronto PhD Thesis, in progress.

[17]E.S.Swanson, private communication.